CrossMark

Study on influence of different mixing rules on the aerosol components retrieval from ground-based remote sensing measurements

Yisong Xie [a,b], Zhengqiang Li [a,b,*], Lei Li [a,b], Ling Wang [c], Donghui Li [a], Cheng Chen [a,b], Kaitao Li [a,b], Hua Xu [a]

[a] State Key Laboratory of Remote Sensing Science, Institute of Remote Sensing and Digital Earth, Chinese Academy of Sciences, Beijing 100101, China
[b] University of Chinese Academy of Sciences, Beijing 100049, China
[c] National Satellite Meteorological Center, China Meteorological Administration, Beijing 100081, China

ARTICLE INFO

ABSTRACT

Mixing states of aerosol components significantly influence the optical, physical and radiative properties of ambient aerosols. The five-component aerosol composition model, including black carbon (BC), brown carbon (BrC), mineral dust (DU), ammonia sulfate (AS) and aerosol water (AW), is improved with considering different mixing rules in this paper. Then we retrieve the volume fractions and column mass concentrations of these aerosol components at Beijing from ground-based AERONET remote sensing measurements, such as refractive index, size distribution, and single scattering albedo. A residual minimization method is used to derive aerosol composition difference under dust, haze and clean conditions at Beijing in 2011. Three mixing rules including Maxwell–Garnett (MG), Bruggeman (BR) and Volume Average (VA) are demonstrated to have significant influences on the aerosol component retrievals. We find that over 50% difference of volume fraction of DU occurs by switching between MG and BR rules. Therefore, applicability of each mixing rule is also investigated. We propose that BR is more suitable for the dust case, MG is better than other two rules for the haze case, and VA is the best choice for the clean case. We also discuss the application scopes of different mixing rules by comparing the recovered aerosol optical parameters with AERONET observations.

© 2014 Elsevier B.V. All rights reserved.

1. Introduction

Aerosol is considered to have significant impacts to global climate and atmosphere environment. It affects climate in both direct and indirect ways (Haywood and Boucher, 2000). Although aerosol scattering at short wavelength is believed to have cooling effects on atmosphere, absorption of aerosols cannot be ignored because the cooling effect of aerosol radiative forcing at the top of atmosphere may change to warming with highly absorbing aerosols (Schuster et al., 2005; Haywood and Shine, 1995; Charlock and Sellers, 1980). Atmospheric models are widely used in estimating global aerosol radiative forcing for

their capability of providing a wide spatial and fine temporal estimate (Wang et al., 2013a). However, inevitable large uncertainties have limited their application (Bond and Bergstrom, 2006; Park et al, 2003). Sato et al. (2003) found that models might need 2–4 times increase for BC emission inventories to match single scattering albedo (SSA) measurements by AERONET (AErosol RObotic NETwork) (Holben et al., 1998). Aerosol is a mixture of solid and liquid components suspended in the atmosphere and radiative impacts of aerosol components are widely varying (Alam et al., 2011), making it difficult to accurately estimate the total aerosol radiative impact. Therefore studies on aerosol component and composition become more and more important for the estimation of aerosol radiative forcing. For example, Srivastava et al. (2012a) derived aerosol optical parameters that are important to radiative forcing

---

* Corresponding author at: No. 20 Datun Road, Beijing 100101, China.
  E-mail address: lizq@radi.ac.cn (Z. Li).

such as aerosol optical depth (AOD) and SSA by aerosol chemical composition measurements and ambient meteorological parameters, and then used them to estimate aerosol direct radiative forcing.

Satellite remote sensing technology provides global aerosol products like AOD and size distribution (Kaufman et al., 2002), but so far it cannot effectively acquire aerosol composition (Ganguly et al., 2009). In situ sampling and laboratory analysis can provide accurate aerosol composition but it is difficult to maintain the natural status of ambient aerosols. Besides, the high time and money cost due to its complexity have limited the application of this technology. In the field of identifying aerosol types and inferring aerosol composition, ground-based remote sensing measurements are becoming promising in recent years for their global coverage and continuous automatic observation, for example, the AERONET. Lee et al. (2010) employed SSA at 440 nm and fine mode fraction (FMF) at 550 nm derived by AERONET to classify global aerosol into several classes. Srivastava et al. (2012b) used the same method to discriminate aerosol types according to their size and radiation absorptivity, and investigated diurnal and spatial variation of aerosol types. Srivastava et al. (2014) also quantified the possible radiative implications of different aerosol types. Aerosol optical and physical properties such as AOD, SSA, refractive indices and size distribution are also useful for aerosol composition retrieval. Schuster et al. (2005) used a three-component aerosol model including black carbon (BC), ammonia sulfate (AS) and water to infer the content and specific absorption of BC. He also investigated the sensitivity of BC content to optical properties. Dey et al. (2006) supplemented partly absorbing components (organic carbon (OC) or mineral dust (DU), depending on observation period) to the model and inferred BC and its specific absorption. Arola et al. (2011) extended the model analogously to acquire absorbing organic carbon (also called as brown carbon, BrC) content. These studies usually ignore DU considering that the spectra of imaginary refractive index of DU and BrC are quite similar. Li Z Q et al. (2013) and Wang et al. (2013a) simulated SSA of BrC and DU and found that differences of SSA spectra in 670–1020 nm can be used to distinguish these two absorbing components. They added SSA information to the inversion scheme and established a five-component model, inferring BrC and DU simultaneously. They further applied this model to the serious haze episodes in Beijing in January 2013, and acquired aerosol composition in haze episodes (Wang et al., 2013b).

Atmospheric particles are a mixture of different components during complex atmospheric chemical and physical processes such as nucleation and condensation. Mixing states of aerosols have significant impacts on light extinction and thus radiative forcing (Lesins et al., 2002; Li L et al., 2013). For example mass absorption efficiency of BC aerosol varies with its mixing state, geometrical morphology and density (Fuller et al., 1999; Schuster et al., 2005; Dey et al., 2006). There are mainly two assumptions of aerosol mixing. One is external mixing in which each aerosol component is physically separated with the others, i.e., each individual particle contains only one type of component. The other is internal mixing, assuming at least two types of aerosol component included in one particle, and the mixture comprehensively reflects physical and chemical properties of all components. Pure external mixing is rare in realistic aerosol. Field measurements show that most aerosol components are internally mixed with others (Lesins et al., 2002) and telescope data illustrates that over 50% of soot and ammonia sulfate aerosols are internally mixed (Schuster et al., 2005). Sometimes initial aerosols are single particles at the source and then develop to internal mixtures during atmospheric chemical reactions. For example, BC, OC and sulfate could be originated from the same combustion process (Yang et al., 2009); however, they might aggregate into a new internal mixture later. Therefore natural aerosol is generally believed to be internally mixed, and varies with its composition, morphology of particles and relative humidity of atmosphere (Schuster et al., 2009; Lesins et al., 2002; Xue et al., 2011).

Internal mixing states of aerosols (here we mainly focus on the mixing rules) have significant impacts on optical and physical properties of aerosol but have not been given adequate attention. Some studies employed one mixing rule to infer aerosol composition. For example, Arola et al. (2011) applied Maxwell–Garnett (MG) effective medium approximation to the retrieval of four-component aerosol model, Wang et al. (2013a) used Volume Average (VA) mixing rule to calculate refractive indices of aerosol mixture in their five-component model. Some studies investigate the differences between mixing rules. For example, Dey et al. (2006) compared Bruggeman (BR) effective medium approximation and MG in composition retrieval but BR was only applied to a two-component model (BC and AS). Schuster et al. (2005) compared external mixing, MG and concentric sphere models and chose MG to infer BC content. Lesins et al. (2002) systematically analyzed the impacts of aerosol mixing states on radiative forcing and compared refractive index simulation under MG, BR and VA mixing rules, but did not applied their results to actual aerosol composition retrieval.

Based on the assumption of internal mixing aerosol, this paper improves the five-component model described in previous work (Li Z Q et al., 2013; Wang et al., 2013a,b) by applying different mixing rules (MG, BR and VA). We then utilize AERONET observation of Beijing site in 2011 to retrieve aerosol composition under selected typical cases (i.e. dust, haze and clean day). We focus on the comparison of retrievals between these mixing rules, and then use simulated refractive index spectra and aerosol absorption optical depth to investigate the applicability of these mixing rules.

2. Data

2.1. AERONET products

AERONET is composed of over 500 observation sites of sun-sky photometer instruments all over the world (until the end of 2012), providing high quality aerosol products (Holben et al., 1998). Sun-sky photometer is capable of automatic observation of direct solar irradiation and also sky radiation with ALMucantar (ALM) and Solar Principle Plane (SPP) geometries. Retrieval results such as refractive indices and size distribution are acquired by ALM geometry, which supplies sky radiation measurements at 28 relative azimuth angles but a fixed solar zenith, almost covering the entire almucantar. Symmetry criteria of ALM might screen some invalid measurements but at least 21 azimuth angles are needed for the retrieval accuracy. AERONET inversion method

(Dubovik and King, 2000; Dubovik et al., 2006) acquires aerosol optical properties by measuring direct solar irradiation and sky radiation at multi scattering angles. Based on optimal matching spectral and angular sky measurements this method can simultaneously solve imaginary and real refractive indices at the scanning wavelengths (440, 670, 870 and 1020 nm) and volume size distribution for 22 particle radii between 0.05 and 15 μm. The accuracy of fine mode dominated (0.1–7.0 μm) size distribution is 15–25%, while for size less than 0.1 or larger than 7.0 μm the accuracy is 25–100%. The accuracy of real refractive index is expected to be 0.04; the accuracy of imaginary refractive index is 30–50% for AOD at 440 nm larger than 0.4 (Dubovik et al., 2000). We use quality assured AERONET level 2.0 products (AOD at 440 nm > 0.4) in this work to retrieve aerosol composition, including refractive index, volume size distribution, and SSA.

2.2. Case selection

We select Apr 16, Oct 29 and Dec 19 of 2011 respectively as typical dust, haze and clean condition cases in this paper by considering some criteria and employ AERONET products on these days in our retrieval. For selection of dust case, we apply the criterion proposed by Dubovik et al. (2002): Ångström Exponent (AE) ≤ 0.6 and AOD (1020 nm) ≥ 0.3. For selection of haze case, we use the three-parameter criterion proposed by Li Z Q et al. (2013): relative humidity (RH) <90%, AOD (440 nm) > 1.0 and AE > 1.0. And for selection of clean case, we simply use AOD as the criterion: AOD (440 nm) < 0.7, the multi-year average of AOD (440 nm) from 2001 to 2012 in AERONET Beijing site, and AOD (440 nm) > 0.4 (for assuring retrieval quality of urban-industrial aerosol).

Fig. 1 shows daily average lognormal volume size distribution of the typical dust, haze and clean case and Table 1 shows related AERONET retrieval parameters, demonstrating good representativeness of the selected cases. The dust case has similar size distribution and SSA spectra (not shown here) to dust aerosol model derived at Cape Verde site (Dubovik et al., 2002) where AE was 0.36, close to our dust case. The size distribution of the selected haze case is quite close to that of haze episodes in Beijing winter as described

Table 1
AERONET retrievals on the selected cases (daily average). "±" indicates standard deviation.

Selected case	Apr 16 2011	Oct 29 2011	Dec 19 2011
Aerosol condition	Dust	Haze	Clean
Number of measurements	7	3	5
AOD (440 nm)	0.93 ± 0.21	1.93 ± 0.39	0.48 ± 0.04
FMF (440 nm)	0.41 ± 0.07	0.94 ± 0.01	0.89 ± 0.01
AE (440–870 nm)	0.44 ± 0.12	1.26 ± 0.08	1.39 ± 0.02
SSA (440 nm)	0.83 ± 0.03	0.94 ± 0.01	0.87 ± 0.01
Total volume (μm³/μm²)	0.72 ± 0.08	0.41 ± 0.07	0.13 ± 0.02
VFMF	0.06 ± 0.01	0.64 ± 0.03	0.46 ± 0.03

by Li Z Q et al. (2013), ignoring the differences of total volume concentration of aerosol (related to AOD). Both haze cases have similar aerosol parameters such as SSA, AE and fine-mode fraction of AOD (FMF), which indicates aerosol absorbing/scattering properties, particle size, and extinction ratio of fine mode aerosol, respectively. The size distribution of clean case is quite like that of Mexico City model (Dubovik et al., 2002) which also belongs to urban/industrial aerosol type only with larger AOD. Besides, the fine-mode fraction in volume (VFMF) of the clean case is similar to VFMF in clean condition of Beijing winter (e.g. Xie et al., 2013).

In dust case AE is 0.44 ± 0.12 and VFMF is 0.06 ± 0.01, indicating the dominated coarse-mode aerosol of size distribution (Eck et al., 2005), as also shown in Fig. 1. The relatively low FMF (0.41 ± 0.07) illustrates the stronger extinction of coarse-mode aerosol than fine-mode in dust case. Aerosol absorption of dust case is the strongest among the three cases, indicated by the small SSA (440 nm), about 0.83 ± 0.03. On the contrary, AE (as well as VFMF and size distribution) and FMF in haze case show clearly fine-mode aerosol dominating both size distribution and light extinction (Kang et al., 2013). Also, the large SSA of haze case (0.94 ± 0.01) indicates the relatively weak absorption (probably due to the much faster growth of scattering coefficient than absorbing coefficient), in accordance with other studies (Yan et al., 2008; Min et al., 2009; Liu et al., 2013). In clean case VFMF is about 0.46 ± 0.03, showing that volume concentrations of both modes are
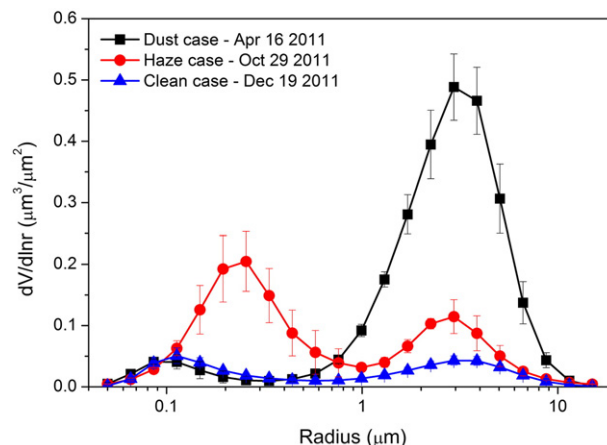

Fig. 1. Aerosol volume size distributions of the three typical cases. Error bar shows standard deviation of daily average.

comparable although coarse-mode aerosol is slightly stronger, agreeing with some previous studies (Yu et al., 2012; Xie et al., 2013). We notice that light extinction of aerosol in haze case is much larger than that in other two cases, which can be explained by the dramatically increased scattering aerosols. Note that the total volume concentration of aerosol in dust case exceeds that of haze case due to much larger size of dust particles.

3. Retrieval method

3.1. Aerosol composition model

Black carbon, mineral dust, organic materials and scattering matters are common components of continental aerosols. Sea salt is also a part of aerosol composition at submaritime regions. Aerosol water is another significant component
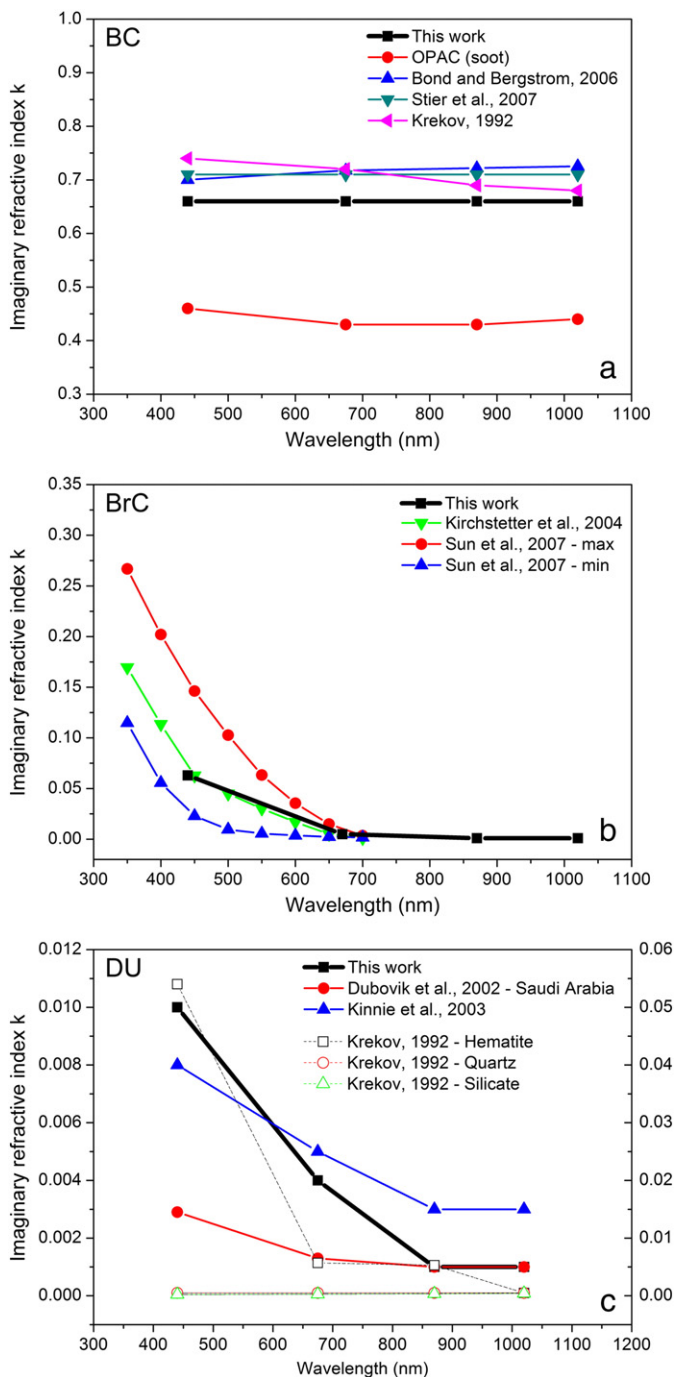

Fig. 2. Spectral imaginary refractive indices of absorbing components in literatures (a) BC, (b) BrC, and (c) DU. The black thick lines indicate *k* values used in this work. Dash lines in (c) indicate main constituents of DU particles (right axis).

except for aerosols at drought and desert regions. Fossil combustion and motor vehicle exhaust are the main sources of black carbon (BC) (Safai et al., 2013), which is an important absorbing component of Beijing aerosol. Scattering aerosols contain sulfate and nitrate, large part of which come from gas-to-particle conversion of polluting gases like sulfur dioxide and nitric oxide mainly from anthropogenic activities (e.g. fossil combustion) (Kai et al., 2007). Note that scattering aerosol is often composed of many species, whose real refractive indices mainly distribute from 1.51 to 1.55. Ammonia sulfate (AS) takes up about 16–54% of submicron aerosol mass and its real refractive index is 1.53 (Wang et al., 2013a), thus we can simply use it as delegate of scattering aerosols. Mineral dust (DU) mainly comes from remote dust sources and local fly ash emission (e.g. construction and traffic dust). Beijing is located near Otindag Sandy Land, one of the main dust sources of North China. Volume fraction of coarse-mode aerosol of Beijing is generally 50% (Eck et al., 2010) and surface sampling research shows similar results (Yuan et al., 2008). Therefore mineral dust should be treated as an important component of Beijing aerosol (Zhao et al., 2007). Organic matters have complex origins (Bi et al., 2008), such as combustion products, volatile organic compound (VOC) and natural organic matter (e.g. pollen). Industrial combustion emission and biomass burning emission are the main sources of BrC (Bahadur et al., 2012), which can be used as representation of absorbing organic aerosols in Beijing (Wang et al., 2013a). Aerosol water (AW) is a critical component of urban type aerosol, especially under haze pollution, when atmospheric water content is considerably high (Wang et al., 2013b). Sea salt can be safely ignored in our model because Beijing is far from sea and there's almost no southeast monsoon bringing sea salt component to Beijing during the research periods. According to the above analysis of aerosol sources, the aerosol composition model used in this paper contains five components: BC, BrC, DU, AS and AW.

3.2. Optical properties of aerosol components

BC, BrC and DU are absorbing aerosols (Arola et al., 2011). BC is an extremely strong absorbing component that has big influence on aerosol optical properties although it generally occupies no more than 5% of atmospheric aerosol in mass (Lesins et al., 2002). BC is very important as it may reduce the direct radiative effect of sulfate aerosols by 50–100% (Schuster et al., 2005). Imaginary refractive index (k) of BC is much larger compared with other components, for example, k at 440 nm is 0.66 (Bergstrom, 1972), about 10 times than that of BrC (0.063) and 60 times than that of DU (0.01) at same wavelength. Another obvious absorbing characteristic of BC is that its k shows very little spectral dependency, as shown in Fig. 2(a).

Increased absorption at 440 nm, often found in ground-based aerosol observation, can be attributed to the existence of partly absorbing components like BrC and DU, considering the k spectral independency of BC (Derimian et al., 2008). BrC has relatively weak absorption compared to BC, however, its k spectra show a prominent increase at short wavelength, i.e. from ultraviolet to blue (Wagner et al., 2012; Bahadur et al., 2012; Feng et al., 2013), as shown in Fig. 2(b). DU is another partly absorbing aerosol component existing extensively in the

global atmosphere. Fig. 2(c) shows that k spectra of DU are similar to BrC except for much smaller values. The increased absorption at 440 nm of DU is due to hematite, the absorbing constituent in dust particles. The k at 440 nm of hematite is about 0.054, much larger than other constituents like quartz and silicate (0.0005) (Koven and Fung, 2006). The spectral dependency of hematite and that of quartz and silicate is contrastively shown in Fig. 2(c).

AS is a typical scattering aerosol component that has almost no absorption at all wavelengths, illustrated by its extremely low imaginary refractive index (the order of 10^{-7}). The strong scattering of solar direct irradiation makes AS a cooling aerosol (Haywood et al., 1997; Penner et al., 1998). AW does not have light absorption (imaginary refractive index is zero), showing only scattering effect to light.

There is no diagnostic spectral characteristic of real refractive indices (n) of these five components (Wang et al., 2012). BC, BrC, DU and AS are further respectively composed of some species, and fortunately for each type the n values of these species are considerably close, for example, n values of AS species vary from 1.51 to 1.55. The real refractive indices of AW at four wavelengths are as low as 1.33 among observation wavelengths. Table 2 lists refractive indices acquired from literatures.

3.3. Retrieval of aerosol components

3.3.1. Mixing rules

Refractive indices of mixed aerosol can be computed by the index of each component in the model according to a certain mixing rule (Chylek et al., 2000). A suitable mixing rule is selected according to the geometric arrangement of the components in the mixture (Lesins et al., 2002). Different mixing rules have their own applications and sometimes reach to very different refractive indices and thus optical properties. Based on different assumptions of aerosol mixing states, we apply three mixing rules, Maxwell–Garnett (MG) effective medium approximation, Bruggeman (BR) effective medium approximation and Volume Average (VA) mixing rule respectively to investigate their applicability to various situations.

(1) Maxwell–Garnett effective medium approximation should be used for the case of insoluble small particles suspended in solution, which can be modeled as insoluble inclusions embedded within a matrix (Bohren and Huffman, 1983). For example, in the case of black carbon in sulfate haze, sulfate solution is assumed to be matrix which contains separated BC inclusions. Note that matrix could be either liquid or solid particles (Schuster et al., 2005). In our MG aerosol model, AW is treated as the matrix and the other four components are inclusions. We compute MG effective dielectric function ε_{MG} by

$$\varepsilon_{MG}(\lambda) = \varepsilon_m(\lambda) \left[1 + \frac{3 \sum f_j \left(\frac{\varepsilon_j(\lambda) - \varepsilon_m(\lambda)}{\varepsilon_j(\lambda) + 2\varepsilon_m(\lambda)} \right)}{1 - \sum f_j \left(\frac{\varepsilon_j(\lambda) - \varepsilon_m(\lambda)}{\varepsilon_j(\lambda) + 2\varepsilon_m(\lambda)} \right)} \right] \quad (1)$$

Table 2
Refractive indices of five components used in the retrieval (Li Z Q et al., 2013).

Component	Imaginary refractive index k				Real refractive index n
	440 nm	670 nm	870 nm	1020 nm	440–1020 nm
BC	0.66	0.66	0.66	0.66	1.95
BrC	0.063	0.005	0.001	0.001	1.53
DU	0.01	0.004	0.001	0.001	1.57
AS	10^{-7}	10^{-7}	10^{-7}	10^{-7}	1.53
AW	0	0	0	0	1.33

where λ is the available wavelengths of AERONET products, i.e. 440, 670, 870 and 1020 nm, f_j indicates the volume fractions of the four inclusions, and ε_m and ε_j are dielectric constants of matrix and inclusions, respectively. Real refractive index n and imaginary refractive index k at each wavelength can be computed by dielectric constant (complex number), following

$$n(\lambda) = \sqrt{\frac{\sqrt{\varepsilon_r^2(\lambda) + \varepsilon_i^2(\lambda)} + \varepsilon_r(\lambda)}{2}} \qquad (2)$$

$$k(\lambda) = \sqrt{\frac{\sqrt{\varepsilon_r^2(\lambda) + \varepsilon_i^2(\lambda)} - \varepsilon_r(\lambda)}{2}} \qquad (3)$$

where ε_r and ε_i are real and imaginary parts of dielectric constant.

(2) Bruggeman effective medium approximation treats all components in the mixture equally and does not distinguish inclusions and matrix. It is suitable for the case of a mixture of random insoluble particles where the dry components are interspersed (Bohren and Huffman, 1983). BR dielectric function ε_{BR} can be calculated by solving the equation

$$\sum f_j \frac{\varepsilon_j - \varepsilon_{BR}}{\varepsilon_j + 2\varepsilon_{BR}} = 0. \qquad (4)$$

(3) Volume average mixing rule, which can avoid complex computation of dielectric function, is based on the assumption that all components are uniformly mixed. The simplicity makes VA as the first choice to calculate refractive indices of mixed aerosol in many studies (Wang et al., 2013a; Li Z Q et al., 2013; Koven and Fung, 2006). Refractive index of each component is weighed by its volume fraction and then summed up to acquire the refractive indices of aerosol mixture as the following:

$$n(\lambda) = \sum f_j n_j(\lambda) \qquad (5)$$

$$k(\lambda) = \sum f_j k_j(\lambda) \qquad (6)$$

where n_j and k_j respectively indicate real and imaginary part of refractive index of each component.

3.3.2. Residual minimization method

Residual minimization is to search for the optimal combination of volume fractions of the five components according to the comparison between the simulation and the AERONET observation. We first assume volume fraction of each component and compute real and imaginary refractive indices based on a mixing rule as described in Section 3.3.1. Then we acquire different value of SSA between 670 and 870 nm, *dSSA*, which helps to distinguish BrC from DU (Wang et al., 2013a), using mass absorption efficient (MAE) and mass density (ρ) (both shown in Table 3) of absorbing components and also AOD and total volume. We compare the simulated n, k, and *dSSA* with the corresponding AERONET observation, and when residual χ^2 between simulation and observation is minimized, the components are considered as retrieval results:

$$\chi^2 = \sum_{s=1}^{4} \frac{\left(n_s^{meas} - n_s^{cal}\right)^2}{n_s^{meas}} + \sum_{s=1}^{4} \frac{\left(k_s^{meas} - k_s^{cal}\right)^2}{k_s^{meas}} + \frac{\left(dSSA^{meas} - dSSA^{cal}\right)^2}{|dSSA^{meas}|}$$

$$(7)$$

where the superscripts *meas* and *cal* denote AERONET observed and simulated parameters respectively, and subscript s indicates the wavelengths used in the retrieval process. The retrieved volume fraction of each component can be further transformed to column mass concentration *col_mass* (in g/m^2) as

$$col\_mass_j = f_j * V_{total} * \rho_j = f_j * \rho_j * \int \frac{dV}{d\ln r} d\ln r \qquad (8)$$

where V_{total} is the total volume of aerosol by integrating the volume size distribution (dV/dln$r$), and ρ_j denotes densities of five components. The detailed process of retrieval method has been described in previous publications (Li Z Q et al., 2013; Wang et al., 2013a), and this paper improves the inversion scheme by applying different mixing rules, as shown in Fig. 3.

4. Results

4.1. Impacts of mixing rules to the retrieval

In this section we show the retrieved volume fraction and column mass concentration (in mg/m^2) of aerosol components in the typical cases. Dust condition is characterized by high level of dust particles and low water content. As shown in Fig. 4(a) and (d), in dust case the retrieved AW contents under the three mixing rules are all equal to zero. For BR and VA rules, volume fraction of BC is about 0.1%, while for MG

Table 3
Physical parameters of components in the retrieval process (Li Z Q et al., 2013).

Aerosol component	Density (g/cm^3)	Mass absorption efficiency (m^2/g)			
		440 nm	675 nm	870 nm	1020 nm
BC[a]	2.0	12.5	8.14	6.32	/
BrC[a]	1.8	0.921	0.067	0.050	/
DU[a]	2.6	0.104	0.045	0.045	/
AS	1.76	/	/	/	/
AW	1.0	/	/	/	/

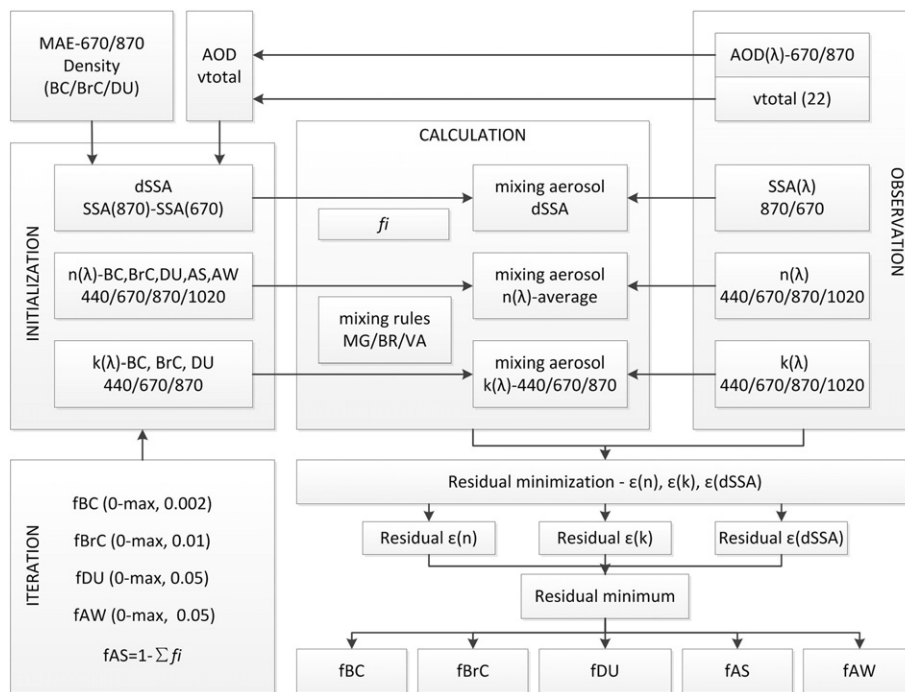[a] Denotes absorbing components.

Fig. 3. Flowchart of the improved aerosol component retrieval method.

rule BC content is a little higher, about 0.49%. Volume fraction of BrC is about 3–6% for the three mixing rules, showing no significant difference. The main composition differences related to mixing rules are found to be DU and AS. The fraction of coarse-mode particles can be related to DU content to a certain extent considering that the majority of DU aerosols are coarse particles with radius larger than 1 μm (Dubovik et al., 2002). The retrieved volume fractions of DU are 80% (BR), 61% (VA) and 25% (MG) while the coarse-mode fraction of dust case is 94%. Therefore we think that BR is better than VA and MG for dust case. The retrieved DU content by BR is consistent with the four-component aerosol model study (Wang et al., 2012). We notice that the retrieved AS content under MG is abnormally high (about 70%) compared with other two cases, and this can be attributed to MG's large underestimation of DU as shown by Fig. 4(a).

Compared with dust case, AW and AS contents in haze case are significantly increased (Li Z Q et al., 2013; Xie et al., 2013). From Fig. 4(b) and (e) we can see that BC content is about 0.6% (5 mg/m²) under MG and VA in haze case, higher than those in dust case. The BrC content acquired by MG and VA is about 2–4% (17–30 mg/m²), equivalent to the BrC level of other researches (Arola et al., 2011; Wang et al., 2013b). However, BC retrieved from BR is smaller (1.58 mg/m²) while BrC is larger (57 mg/m²). Some researches indicate that DU occupies a considerable large fraction at haze episode in Beijing, about 30–40% (Li Z Q et al., 2013; Wang et al., 2013b), in accordance with DU retrieved from MG and BR but far larger than that from VA (only 5%) in the present study. Under haze pollution the scattering aerosol AS has an obvious increase (Yan et al., 2008; Wei et al., 2013). Our retrieval of AS is 133, 335 and 279 mg/m² respectively for MG, BR and VA, and MG retrieval shows good consistency with the AS content at haze episodes in

Jan 2013 in Beijing (~132 mg/m² from Wang et al., 2013b) while BR and VA seem to overestimate it. Increased water content is another significant feature of haze as proved by some studies (Yu et al., 2012; Min et al., 2009). AW retrieved from MG and VA is about 45% that relates to high RH, much larger than that in dust and clean cases. However, AW is substantially underestimated by BR according to which AW is only 10%, even lower than the level on clean day. From above analysis we conclude that MG mixing rule is better than the other two for aerosol composition retrieval in haze case.

In clean case both AOD and total volume of aerosols are relatively small, as shown in Table 1, thus the absolute mass differences between mixing rules are small compared to those in other two cases, although volume fraction of components shows some obvious deviations. From Fig. 4(c) and (f) we can see that BC contents from different rules are similar, about 1.2% (3 mg/m²), agreeing well with Wang et al. (2013b), who claimed that BC was about 4 mg/m² on clean days of Beijing. BrC retrieved from MG and VA is about 20 mg/m², close to the lower limit of heavy haze pollution. But BR retrieval of BrC (51 mg/m²) is highly overestimated, more than twice the values of other cases, almost reaching to the typical level of heavy haze pollution. DU is a common aerosol component in Beijing and there are a certain amount of dust particles even in clean condition (Yuan et al., 2008). The volume fraction of DU retrieved under MG and VA is respectively 62% and 43%, close to the coarse-mode fraction of this case (54%). However, BR retrieval of DU is only 25%, which is probably attributed to its overestimation of BrC. Scattering aerosols make important contributions to mass of urban aerosols and to the light extinction. The VA and BR retrievals of AS contents are about 70 mg/m² which matches AS content of other study (Wang et al, 2013b), and MG
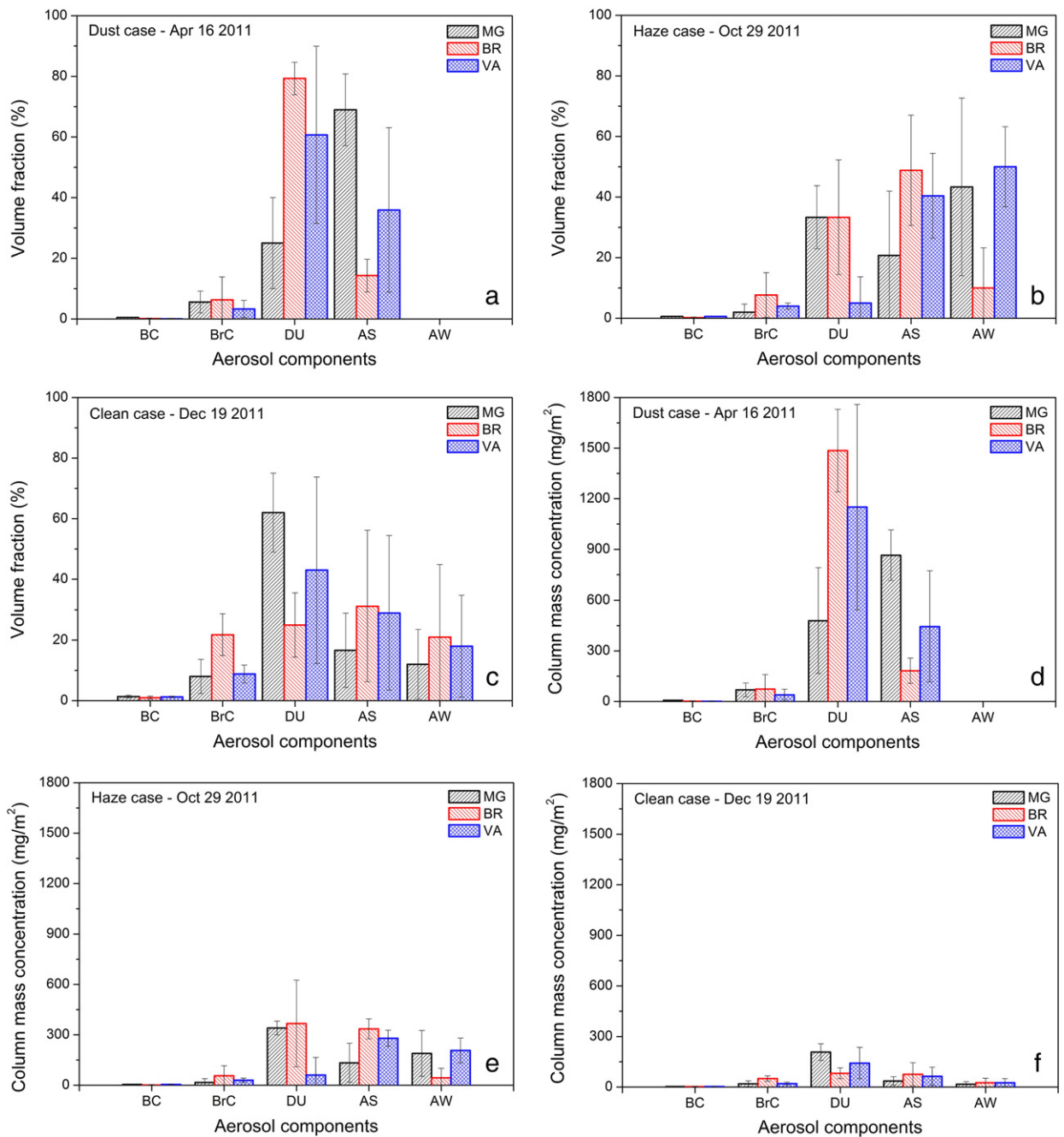
Fig. 4. Retrieval of volume fractions (left panels) and mass column concentrations (right panels) of aerosol components using different mixing rules.

retrieval of AS is slightly smaller. In clean case, AW content (about 12–20%) lies between haze and dust cases, and there is no obvious deviation between the mixing rules. As we have discussed above, VA is the most appropriate choice for composition retrieval for clean case.

We find significant impacts of mixing rules to the retrieval. In dust case, the volume fraction difference of DU from MG and BR retrievals is about 54% and that of AS is 55%. In haze case, the volume fraction difference of AW from BR and VA retrievals reaches to 40%, and the difference between MG and

BR retrievals of AS is 28%. In clean case, volume fraction difference of DU from MG and BR retrievals is 37%. These deviations indicate that DU and AS have largest difference when employing different mixing rules, i.e. these two components are the most likely to be affected by mixing rules. The choice of mixing rules affects retrieval to a great extent because they have significant influence on the calculation of refractive indices, which provide much of the information to the inversion, as Eq. (7) shown. The applicability of the mixing rules will be further discussed in Section 5.

4.2. Comparison to AERONET observation

In order to validate our results, we simulate refractive indices and aerosol absorption optical depth (AAOD) of the mixed aerosol using the retrieved volume fraction of components, and compare them with corresponding AERONET observation.

Fig. 5 shows the observed spectra of imaginary (k) and real (n) refractive index acquired by AERONET and the simulation using the retrieved component volume fractions, which are calculated according to MG, BR and VA mixing rules, respectively. We can see that the simulated k of different mixing rules (Fig. 5, solid lines) shows similar spectral characteristics with observation, i.e. high at 440 nm and low and invariant at
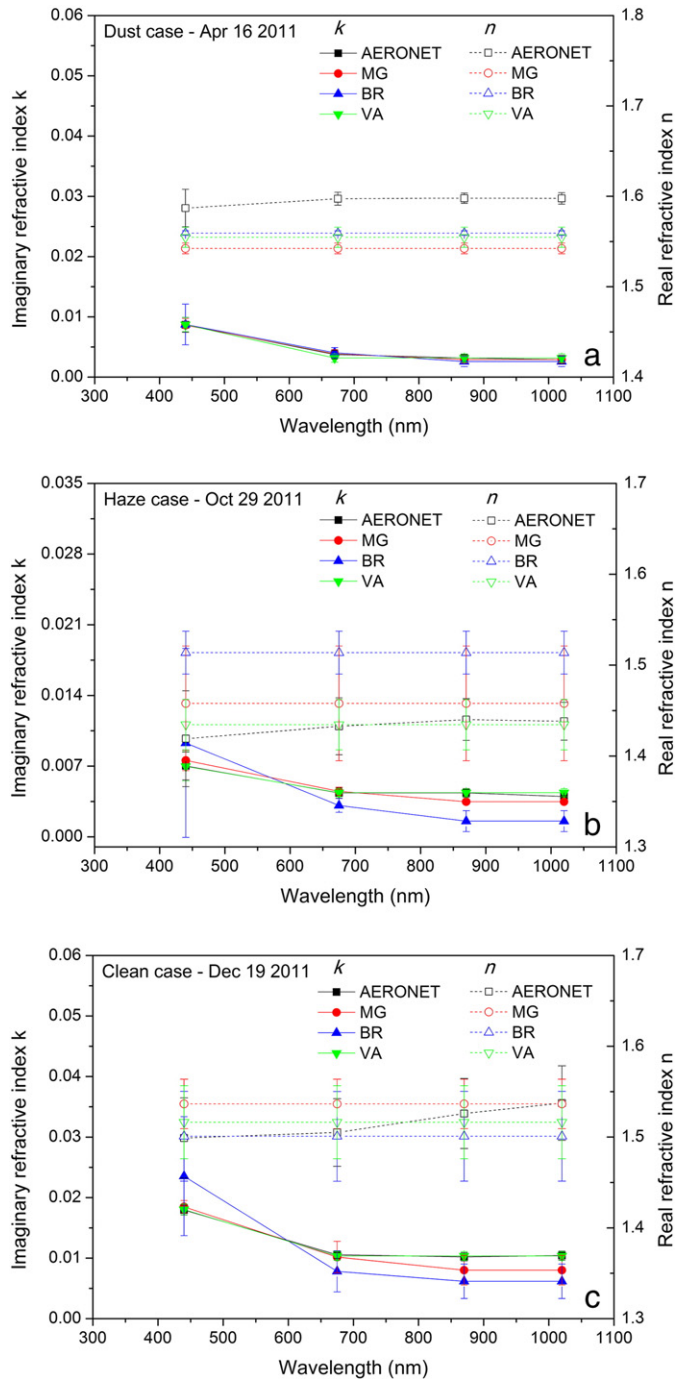

Fig. 5. Comparison between simulated and observed refractive index spectra under different mixing rules. (a) Dust case, (b) haze case and (c) clean case.

the other wavelengths. In dust case, the k spectra acquired from mixing rules are all very close to observation with deviations no more than 10%. Note that we have stated the big underestimation of DU of MG retrieval in dust case (about 55%) in Section 4.2, but from Fig. 5(a) there is no notable k difference between BR and MG retrievals. This can be explained by the small overestimation of BC considering BC has much larger k than DU. In haze case, VA and MG simulations have good agreements and the deviations are 3% and 11%, respectively. However, BR simulation leads to an extremely large deviation, about 47%, which is probably caused by its misestimating of other components. For example, the higher k at 440 nm is due to overestimation of BrC and the low k values at other wavelengths can be attributed to underestimation of BC. In clean case, VA simulation has the best agreement with observation, and the simulating deviation is only 1%, much smaller than MG and BR (about 35%).

We also notice some differences between mixing rules from real refractive indices (Fig. 5, dash lines). In dust case, the best match to observed n spectrum is BR simulation, and the deviation is about 2.2%. The n values simulated by MG and VA are slightly smaller with deviations of 3.3% and 2.5%, respectively. In haze case the deviation between BR simulation and observation is larger than that of MG and VA, probably due to its underestimation of AW. In clean case, VA simulates the best n spectra, while MG simulation is a little higher (1.5%) and BR simulation is a little lower (1.0%). We need to mention that our aerosol model assumes spectrally independent real refractive index, thus the simulated n at all wavelengths are almost the same. However, n values of AERONET may have differences with wavelengths. The comparison between observed and simulated refractive index spectra illustrates the applicability of different mixing rules, i.e. BR is more suitable for the dust case, MG has better effect than the other two rules for the haze case, and VA is the best choice for the clean case.

Simulated AAOD can be acquired by using the retrieved mass concentration of absorbing components (BC, BrC and DU) and their mass absorption efficiencies (Table 3). AERONET AAOD is calculated using AOD and SSA. Fig. 6 shows the comparison between observation and simulations using different mixing rules in different cases. We can see that the simulated

AAOD of the three mixing rules are generally close to observation and accordingly could reflect optical absorption of aerosols in the selected cases. MG simulation has the lowest precision for dust case, about 33% deviated from observation, probably due to its overestimation of BC, while BR and VA have better performance (deviations are respectively 18% and 13%). In the haze case, AAOD simulated by MG and BR are much closer to observation (3% and 2% deviations, respectively) than VA (12%), and the latter might have some underestimation of DU. VA simulation, as expected, best matches observed AAOD in clean case with the deviation of 19% while MG and BR simulations are higher than observation (deviated from 33% and 39% respectively), probably due to the overestimation of DU and BrC. Note that the assessments based on AAOD are not in the same parameter space with that based on refractive index as discussed before, however, we still arrive at the same conclusion that MG, BR and VA mixing rules are respectively suitable for inferring the composition in the selected haze, dust and clean case, as Section 4.1 concluded.

5. Discussion

It is illustrated that differences between mixing rules can cause important uncertainties to the retrieval in Section 4.1. Lesins et al. (2002) showed that the difference between these mixing rules is related to the disparity in the individual refractive indices. And this can partly explain the significant differences in the retrieved composition between mixing rules, since the real and imaginary parts are highly varying in the model (at 440 nm, the extreme values of refractive indices are 1.57 (DU) and 1.33 (AW) for real part, while 0.66 (BC) and 0 (AW) for imaginary part). It is necessary to choose a proper mixing rule for aerosol composition model because in the calculation of aerosol optical properties it determines the refractive indices and probably the optically equivalent size of particles. They could seriously affect extinction coefficient and scattering coefficient, and thus have significant impacts on optical properties of aerosol mixture such as AOD, SSA and asymmetry parameter. In addition, uncertainties of these radiatively important optical properties are one of the possible error sources of radiative forcing estimation. Atmospheric radiative forcing is therefore highly associated with
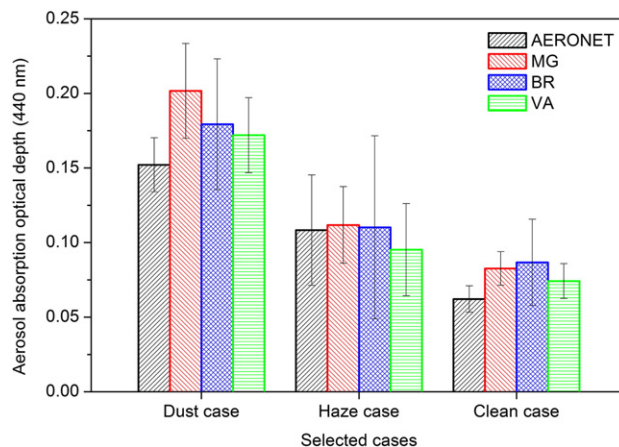

Fig. 6. Comparison between simulated and observed AAOD (440 nm) under different mixing rules.

mixing state of aerosols (Srivastava et al., 2014). For example, Lesins et al. (2002) tested impacts of aerosol mixing states on radiative forcing through a simplified aerosol composition model and concluded that the radiative forcing was so sensitive to the mixing state assumption that the difference caused by mixing state alone can be comparable to the level of anthropogenic aerosol direct forcing.

The comparisons of retrievals show that the performance of each mixing rule could be varying under different aerosol mixing states. Model assumptions of each mixing rule probably cause these differences. The applicable conditions of MG are: i) insoluble particles with random distribution embedded in homogeneous matrix, ii) spherical inclusions and particles, and iii) clear definitions of inclusions and matrix, noticing that ε_m and ε_j are not interchangeable in Eq. (1). Thus MG is suitable for the cases where RH is relatively high or matrix material is significantly more than inclusions. Haze case matches well with MG conditions that the high water content in haze can be effective matrix with inclusions like BC and BrC embedded in and particles are closer to sphere at high RH condition (noting the increased sphericity of haze aerosol). However, MG does not perform as good in dust case, and this is probably due to the very low RH (also can be seen from the retrieved water content in Fig. 4), while Eq. (1) requires considerable amount of aerosol water. The applicable conditions of BR are: i) dry and insoluble particles and ii) randomly inhomogeneous distribution. Note that it's not necessary to clearly define inclusions and matrix for BR mixture and thus ε_j in Eq. (4) is interchangeable, and BR does not have any restriction to particulate shapes. BR is suitable for the case of low RH and dry components interspersed in the mixture (but are not embedded in a matrix). Dust case applies to BR conditions well thanks to the very low RH and randomly mixed dry particles with various shapes. Unlike MG, BR does not strictly apply to a particulate medium given that it's difficult to decide which component is the inclusion and which component is the surrounding medium in the mixture (Bohren and Huffman, 1983). Therefore BR does not work well for haze case considering the relatively high RH and the dominant particulate medium. VA is suitable for a homogeneously mixed aerosol case in which neither dry/wet status of aerosol nor particulate shape is strictly required, in accordance with situation of the clean case in our research. And that is why VA has better performance for clean case than MG and BR. We can also conclude from comparisons between mixing rules (as shown in Figs. 5 and 6) that VA has wider application range than the other two rules, while MG and BR are more efficient respectively for haze and dust case. We should choose the appropriate mixing rule before investigating aerosol optical and radiative properties, and a prior knowledge of aerosols, for example the major types of aerosol (e.g. DU or AS dominating) and status of ambient atmosphere (like RH), can be very helpful.

6. Conclusion

Based on aerosol optical and physical properties acquired from AERONET, we employ the five-component aerosol model that contains BC, BrC, DU, AS and AW to retrieve volume fraction and column mass concentration of aerosol components, under three selected typical cases at Beijing in 2011, which effectively represent the corresponding ambient aerosol conditions. We improve the retrieval model by applying different mixing rules according to a prior knowledge to illustrate the impacts of mixing rules on the aerosol component retrieval. We find that mixing rules have significant impacts on composition retrieval due to the different calculation methods of refractive indices. In dust case, there is over 50% difference of DU volume fraction between MG and BR retrievals. In haze case AW retrieved from BR and VA has a deviation of 40% in volume. In clean case the volume fraction difference of DU between MG and BR retrievals is about 37%.

The simulations of aerosol optical parameter are employed to evaluate application scopes of the mixing rules as well. For real part of refractive index in dust case BR performs better than MG and VA, while for imaginary part all rules obtain similar k spectra versus the observation. In haze case, VA and MG simulations, for both real and imaginary refractive index parts, are better than BR. And in clean case refractive indices simulated by VA are closest to the observed ones. From aerosol absorption characteristic, AAOD, we also obtain the similar conclusion that MG, BR and VA mixing rules are suitable for composition retrieval respectively in haze, dust and clean case. In addition, it is illustrated that VA has a wider application while MG and BR are mainly suitable for haze and dust case respectively. The next work will focus on developing an automatic mixing rule choosing strategy applied to current aerosol composition retrieval scheme based on observation quantities like absorbing Ångström exponent (Bergstrom et al., 2007) and size distribution.

References

Alam, K., Trautmann, T., Blaschke, T., 2011. Aerosol optical properties and radiative forcing over mega-city Karachi. Atmos. Res. 101, 773–782.

Arola, A., et al., 2011. Inferring absorbing organic carbon content from AERONET data. Atmos. Chem. Phys. 11, 215–225.

Bahadur, R., Praveen, P.S., Xu, Y.Y., Ramanathan, V., 2012. Solar absorption by elemental and brown carbon determined from spectral observations. Proc. Natl. Acad. Sci. U. S. A. 109, 17366–17371.

Bergstrom, R.W., 1972. Predictions of spectral absorption and extinction coefficients of an urban air-pollution aerosol model. Atmos. Environ. 6, 247–258.

Bergstrom, R.W., et al., 2007. Spectral absorption properties of atmospheric aerosols. Atmos. Chem. Phys. 7, 5937–5943.

Bi, X.H., Simoneit, B.R.T., Sheng, G.Y., Ma, S.X., Fu, J.M., 2008. Composition and major sources of organic compounds in urban aerosols. Atmos. Res. 88, 256–265.

Bohren, C.F., Huffman, D.R., 1983. Absorption and Scattering of Light by Small Particles. John Wiley, Hoboken, N. J.

Bond, T.C., Bergstrom, R.W., 2006. Light absorption by carbonaceous particles: an investigative review. Aerosol Sci. Technol. 40, 27–67.

Charlock, T.P., Sellers, W.D., 1980. Aerosol effects on climate — calculations with time-dependent and steady-state radiative-convective models. J. Atmos. Sci. 37, 1327–1341.

Chylek, P., Videen, G., Geldart, W., Dobbie, J.S., Tso, W., 2000. Effective medium approximation for heterogeneous particles. In: Mishchenko, M.

(Ed.), Light Scattering by Nonspherical Particles: Theory, Measurements and Geophysical Applications. Academic, San Diego, Calif., pp. 273–308.

Derimian, Y., et al., 2008. The role of iron and black carbon in aerosol light absorption. Atmos. Chem. Phys. 8, 3623–3637.

Dey, S., Tripathi, S.N., Singh, R.P., Holben, B.N., 2006. Retrieval of black carbon and specific absorption over Kanpur city, northern India during 2001–2003 using AERONET data. Atmos. Environ. 40, 445–456.

Dubovik, O., King, M.D., 2000. A flexible inversion algorithm for retrieval of aerosol optical properties from Sun and sky radiance measurements. J. Geophys. Res.-Atmos. 105, 20673–20696.

Dubovik, O., et al., 2000. Accuracy assessments of aerosol optical properties retrieved from Aerosol Robotic Network (AERONET) Sun and sky radiance measurements. J. Geophys. Res.-Atmos. 105, 9791–9806.

Dubovik, O., et al., 2002. Variability of absorption and optical properties of key aerosol types observed in worldwide locations. J. Atmos. Sci. 59, 590–608.

Dubovik, O., et al., 2006. Application of spheroid models to account for aerosol particle nonsphericity in remote sensing of desert dust. J. Geophys. Res.-Atmos. 111.

Eck, T.F., et al., 2005. Columnar aerosol optical properties at AERONET sites in central eastern Asia and aerosol transport to the tropical mid-Pacific. J. Geophys. Res.-Atmos. 110.

Eck, T.F., et al., 2010. Climatological aspects of the optical properties of fine/coarse mode aerosol mixtures. J. Geophys. Res.-Atmos. 115.

Feng, Y., Ramanathan, V., Kotamarthi, V.R., 2013. Brown carbon: a significant atmospheric absorber of solar radiation? Atmos. Chem. Phys. Discuss. 13, 2795–2833.

Fuller, K.A., Malm, W.C., Kreidenweis, S.M., 1999. Effects of mixing on extinction by carbonaceous particles. J. Geophys. Res.-Atmos. 104, 15941–15954.

Ganguly, D., et al., 2009. Inferring the composition and concentration of aerosols by combining AERONET and MPLNET data: comparison with other measurements and utilization to evaluate GCM output. J. Geophys. Res.-Atmos. 114.

Haywood, J., Boucher, O., 2000. Estimates of the direct and indirect radiative forcing due to tropospheric aerosols: a review. Rev. Geophys. 38, 513–543.

Haywood, J.M., Shine, K.P., 1995. The effect of anthropogenic sulfate and soot aerosol on the clear-sky planetary radiation budget. Geophys. Res. Lett. 22, 603–606.

Haywood, J.M., Roberts, D.L., Slingo, A., Edwards, J.M., Shine, K.P., 1997. General circulation model calculations of the direct radiative forcing by anthropogenic sulfate and fossil-fuel soot aerosol. J. Clim. 10, 1562–1577.

Holben, B.N., et al., 1998. AERONET — a federated instrument network and data archive for aerosol characterization. Remote Sens. Environ. 66, 1–16.

Kai, Z., Wang, Y.S., Wen, T.X., Yousef, M., Frank, M., 2007. Properties of nitrate, sulfate and ammonium in typical polluted atmospheric aerosols (PM10) in Beijing. Atmos. Res. 84, 67–77.

Kang, E., Han, J., Lee, M., Lee, G., Kim, J.C., 2013. Chemical characteristics of size-resolved aerosols from Asian dust and haze episode in Seoul Metropolitan City. Atmos. Res. 127, 34–46.

Kaufman, Y.J., Tanre, D., Boucher, O., 2002. A satellite view of aerosols in the climate system. Nature 419, 215–223.

Koven, C.D., Fung, I., 2006. Inferring dust composition from wavelength-dependent absorption in Aerosol Robotic Network (AERONET) data. J. Geophys. Res.-Atmos. 111.

Lee, J., Kim, J., Song, C.H., Kim, S.B., Chun, Y., Sohn, B.J., Holben, B.N., 2010. Characteristics of aerosol types from AERONET sunphotometer measurements. Atmos. Environ. 44, 3110–3117.

Lesins, G., Chylek, P., Lohmann, U., 2002. A study of internal and external mixing scenarios and its effect on aerosol optical properties and direct radiative forcing. J. Geophys. Res.-Atmos. 107.

Li, L., Chen, J.M., Wang, L., Melluki, W., Zhou, H.R., 2013. Aerosol single scattering albedo affected by chemical composition: an investigation using CRDS combined with MARGA. Atmos. Res. 124, 149–157.

Li, Z.Q., et al., 2013. Aerosol physical and chemical properties retrieved from ground-based remote sensing measurements during heavy haze days in Beijing winter. Atmos. Chem. Phys. 13, 10171–10183.

Liu, X.G., et al., 2013. Increase of aerosol scattering by hygroscopic growth: observation, modeling, and implications on visibility. Atmos. Res. 132, 91–101.

Min, M., Wang, P.C., Zong, X.M., Xia, J.R., Meng, X.Y., 2009. Observation and study on aerosol properties in hazy days. Clim. Environ. Res. 14, 153–160.

Park, R.J., Jacob, D.J., Chin, M., Martin, R.V., 2003. Sources of carbonaceous aerosols over the United States and implications for natural visibility. J. Geophys. Res.-Atmos. 108.

Penner, J.E., Chuang, C.C., Grant, K., 1998. Climate forcing by carbonaceous and sulfate aerosols. Clim. Dyn. 14, 839–851.

Safai, P.D., Raju, M.P., Budhavant, K.B., Rao, P.S.P., Devara, P.C.S., 2013. Long term studies on characteristics of black carbon aerosols over a tropical urban station Pune, India. Atmos. Res. 132, 173–184.

Sato, M., et al., 2003. Global atmospheric black carbon inferred from AERONET. Proc. Natl. Acad. Sci. U. S. A. 100, 6319–6324.

Schuster, G.L., Dubovik, O., Holben, B.N., Clothiaux, E.E., 2005. Inferring black carbon content and specific absorption from Aerosol Robotic Network (AERONET) aerosol retrievals. J. Geophys. Res.-Atmos. 110.

Schuster, G.L., Lin, B., Dubovik, O., 2009. Remote sensing of aerosol water uptake. Geophys. Res. Lett. 36.

Srivastava, A.K., Singh, S., Tiwari, S., Bisht, D.S., 2012a. Contribution of anthropogenic aerosols in direct radiative forcing and atmospheric heating rate over Delhi in the Indo-Gangetic Basin. Environ. Sci. Pollut. Res. 19, 1144–1158.

Srivastava, A.K., Tripathi, S.N., Dey, S., Kanawade, V.P., Tiwari, S., 2012b. Inferring aerosol types over the Indo-Gangetic Basin from ground based sunphotometer measurements. Atmos. Res. 109–110, 64–75.

Srivastava, A.K., Yadav, V., Pathak, V., Singh, S., Tiwari, S., Bisht, D.S., Goloub, P., 2014. Variability in radiative properties of major aerosol types: a year-long study over Delhi-an urban station in Indo-Gangetic Basin. Sci. Total Environ. 473–474, 659–666.

Wagner, R., et al., 2012. Complex refractive indices of Saharan dust samples at visible and near UV wavelengths: a laboratory study. Atmos. Chem. Phys. 12, 2491–2512.

Wang, L., et al., 2012. Retrieval of dust fraction of atmospheric aerosols based on spectra characteristics of refractive indices obtained from remote sensing measurements. Spectrosc. Spectr. Anal. 32, 1644–1649.

Wang, L., et al., 2013a. Estimate of aerosol absorbing components of black carbon, brown carbon, and dust from ground-based remote sensing data of sun-sky radiometers. J. Geophys. Res.-Atmos. 118, 6534–6543.

Wang, L., Li, Z.Q., Ma, Y., Li, L., Wei, P., 2013b. Retrieval of aerosol chemical composition from ground-based remote sensing data of sun-sky radiometers during haze days in Beijing winter. J. Remote Sens. 17, 944–958.

Wei, P., et al., 2013. Remote sensing estimation of aerosol composition and radiative effects in haze days. J. Remote Sens. 17, 1021–1031.

Xie, Y.S., et al., 2013. Aerosol optical and microphysical properties in haze days based on ground-based remote sensing measurements. J. Remote Sens. 17, 970–980.

Xue, M., Ma, J.Z., Yan, P., Pan, X.L., 2011. Impacts of pollution and dust aerosols on the atmospheric optical properties over a polluted rural area near Beijing city. Atmos. Res. 101, 835–843.

Yan, P., et al., 2008. The measurement of aerosol optical properties at a rural site in Northern China. Atmos. Chem. Phys. 8, 2229–2242.

Yang, M., Howell, S.G., Zhuang, J., Huebert, B.J., 2009. Attribution of aerosol light absorption to black carbon, brown carbon, and dust in China — interpretations of atmospheric measurements during EAST-AIRE. Atmos. Chem. Phys. 9, 2035–2050.

Yu, X.N., Li, X.M., Deng, Z.R.D., De, Q.Y.Z., Yuan, S., 2012. Optical properties of aerosol during haze-fog episodes in Beijing. Environ. Sci. 33, 1057–1062.

Yuan, H., Zhuang, G.S., Li, J., Wang, Z.F., Li, J., 2008. Mixing of mineral with pollution aerosols in dust season in Beijing: Revealed by source apportionment study. Atmos. Environ. 42, 2141–2157.

Zhao, X.J., et al., 2007. Variation of sources and mixing mechanism of mineral dust with pollution aerosol — revealed by the two peaks of a super dust storm in Beijing. Atmos. Res. 84, 265–279.